Does the Ring Compound $[(CH_3)_2GaNH_2]_3$ Form during MOVPE of Gallium Nitride? Investigations via Density Functional and Reaction Rate Theories

Debasis Sengupta

CFD Research Corporation, 215 Wynn Drive, Suite 501, Huntsville, Alabama 35805

Received: July 24, 2002; In Final Form: September 19, 2002

Gallium nitride (GaN) thin films are grown by metalorganic vapor phase epitaxy (MOVPE). Trimethylgallium (TMG) and ammonia are used as group III and V precursors, respectively. It has been suggested by several past studies that the trimer (or ring compound), $[(CH_3)_2GaNH_2]_3$, is formed in appreciable amounts in the gas phase during the MOVPE of GaN and is ultimately responsible for the growth process. However, recent mass spectrometric studies seem to indicate otherwise. The purpose of this paper is to explore this debatable issue using density functional (DFT) and reaction rate theories. The potential energy surfaces, obtained via DFT calculations, are used for calculation of rate constant as a function of pressure and temperature using quantum Rice−Ramsperger−Kassel theory. These rate constants are then used for calculations of concentrations of various species over a range of the III/V ratio at various temperatures. Our results suggest that the ring compound is negligible and cannot initiate the main pathway for growth of GaN.

Introduction

Group III nitrides have drawn much attention in the past few years due to their unique ability to produce blue-green light. This optical property is now being explored to develop light-emitting diodes (LEDs) and lasers. Of all III nitrides, gallium nitride (GaN) has shown tremendous potential in electronic applications due to its unusually large band gap.[1] Metalorganic vapor phase epitaxy (MOVPE) is the commercial technique of choice for growing single crystalline thin films of these materials. The efficient production of high quality GaN films by MOVPE requires a fundamental understanding of the chemistry underlying the growth process.

Usually, the metal alkyls are used as precursors for the group III metal while ammonia (NH_3) is used as the nitrogen source. The most common problem during the MOVPE of III nitrides is the formation of a stable adduct (i.e., Lewis acid−base complex) between the metal alkyls and the NH_3. This adduct subsequently eliminates hydrocarbons to form oligomers. This reaction is thought to affect the growth and property of film due to the incorporation of particles into the film.[2,3] For GaN growth, trimethylgallium (TMG) is used as the group III precursor. Thon and Kuech[4] reported the $TMG{\cdot}NH_3$ adduct formation and postulated that this adduct transforms into a trimeric form, $[(CH_3)_2GaNH_2]_3$ (also known as "ring compound"), in the gas phase after elimination of CH_4.

$$TMG + NH_3 \rightarrow TMG{\cdot}NH_3 \rightarrow (CH_3)_2GaNH_2 + CH_4$$

$$3(CH_3)_2GaNH_2 \rightarrow [(CH_3)_2GaNH_2]_3$$

This ring compound has been thought to be responsible for GaN growth. Also, this step has been included as one of the main pathways in the mechanisms proposed in the literature, which have been frequently used for the reactor scale modeling growth process,[5−8] and the rate constants were calibrated to reproduce experimental growth rate. Almond et al., on the basis of their experimental results, concluded that a trimeric species can form during the growth of GaN.[9] They performed experiments where the solid crystal was evaporated, and the vapor was found to contain the trimeric species. However, no experiment was performed starting from gas phase TMG and NH_3. Therefore, these results do not confirm the formation of the trimeric species in a typical growth condition of GaN. To our knowledge, there exists no direct experimental evidence of the ring formation to support this postulate. The role of the ring compound in GaN growth cannot be therefore determined conclusively from these observations. A recent mass spectrometric study by Bergman et al.[10] on TMG and NH_3 reactions reveals that the concentration of the trimer is negligible, especially at growth temperature. On the basis of these observations, Bergman et al.[10] conclude that the role of the trimer has been largely overestimated in the past studies. These results cast doubt on whether the trimer at all contributes to the growth process during MOVPE of GaN. Furthermore, Fourier transform infrared (FTIR) analysis and detailed surface studies of the reaction between TMG and NH_3 suggest that TMG and NH_3 are more likely to form oligomers at the surface than in the gas phase.[11] Therefore, computational method, together with large scale reactor modeling, could be helpful in understanding the mechanism of GaN growth.

The goal of the present paper is to study the gas phase reactions between TMG and NH_3 in detail via density functional (DFT) and reaction rate theories. The potential energy surface of various adduct formation reactions has been reported. The potential energy surface of the calculated reactions is then used to calculate the rate constants using the quantum Rice−Ramsperger−Kassel (QRRK)[12−15] theory over a wide range of temperatures and pressures. We then utilize the rate constants to calculate the concentration of the intermediate species at various temperatures by solving a set of ordinary differential equations. Because the formation of the ring compound is only possible from its monomeric form, $(CH_3)_2GaNH_2$, we examined its concentration over a range of temperatures and III/V ratio.

* To whom correspondence should be addressed. Tel: (256)726-4944. Fax: (256)726-4806. E-mail: dxs@cfdrc.com.

10.1021/jp021721i CCC: $25.00
Published on Web 12/04/2002

TABLE 1: Adduct Formation Energy, Energy of the Transition State, and the Product for Reactions of TMG, DMG, and MMG with NH_3[a]

				E_{diss}			
reactions	adduct	TS	product	this work	ref 22	JANNAF	ref 35
$TMG + NH_3$	−12.5	19.7	−17.1				
$DMG + NH_3$	−10.6	20.7	−11.5				
$MMG + NH_3$	−8.2	17.9	−23.2				
$TMG \rightarrow DMG + CH_3$				68.3	59.5	61.3	64.6
$DMG \rightarrow MMG + CH_3$				28.0	35.4	37.0	52.6
$MMG \rightarrow Ga + CH_3$				58.7	77.5	83.5	54.1

[a] Also, the dissociation energies of TMG, DMG, and MMG are shown. The energies are relative to the corresponding reactant(s). Energies are expressed in kcal/mol. TS and E_{diss} refer to the transition state and dissociation energy, respectively. Energies are calculated using the cc-pVTZ basis set using the B3LYP/6-31G** optimized geometries.

Results and Discussion

Quantum Chemistry Calculations. All quantum chemistry calculations were performed using the GAUSSIAN98[16] program package. For the calculation of the activation barrier, the DFT with the Lee−Yang−Parr gradient-corrected correlation functional in conjuction with Becke's three parameter exchange functional (B3LYP) was used.[17] The geometries of the equilibrium molecular structures and the transition states were optimized using 6-31G** basis sets for carbon, hydrogen, and nitrogen. For Ga, the effective core potential (ECP) of Hay-Wadt, which is known as LANL2DZ ECP,[18] was used. To obtain more accurate energies, calculations using the cc-pVTZ basis set on previously optimized geometries were performed. This basis set includes all electrons in the atoms with triple-ζ plus polarization functions. Normal mode analyses for all equilibrium and transition structures were performed. All equilibrium structures were found to have real vibrational frequencies while the transition structures had only one imaginary vibrational frequency corresponding to the reaction coordinate.

Adduct Formation, Methane Elimination, and Unimolecular Decomposition. TMG makes a very stable adduct with NH_3. The binding energy of the adduct is found to be 12.5 kcal/mol. Dimethylgallium (DMG) and monomethylgallium (MMG) also form strong adducts with NH_3. DMG and MMG are formed by successive elimination of one and two methyl groups, respectively, from TMG. The adduct formation energy decreases with a decrease in the number of methyl groups attached to the Ga atom (Table 1) by approximately 2 kcal/mol for elimination of every methyl group. The calculated adduct formation energy for the $TMG{\cdot}NH_3$ complex is approximately 6 kcal/mol lower than that reported by Nakamura et al.[19] However, their reported values do not include zero point energy (ZPE) corrections. The ZPE correction contributes approximately 3 kcal/mol to the adduct formation energy. Moreover, the basis set used by Nakamura et al. is much lower than that in the present calculation. The stability of the complex was attributed to the stabilizing interaction between the lone pair electrons of NH_3 and the lowest unoccupied molecular orbital of TMG. It is to be noted that there is no potential barrier for the adduct formation reactions. This adduct formation reaction was also calculated by Watwe et al.[20] They obtained a value of 20 kcal/mol using DFT with the B3LYP exchange correlation function. However, a lower level basis set 6-31+G** was used for the calculation.

The adducts can undergo a methane elimination reaction to produce $(CH_3)_y$ $GaNH_2$ ($y = 0-2$):

$$Ga(CH_3)_{y+1} + NH_3 \rightarrow Ga(CH_3)_{y+1}{\cdot}NH_3 \rightarrow (CH_3)_y{\cdot}GaNH_2 + CH_4$$

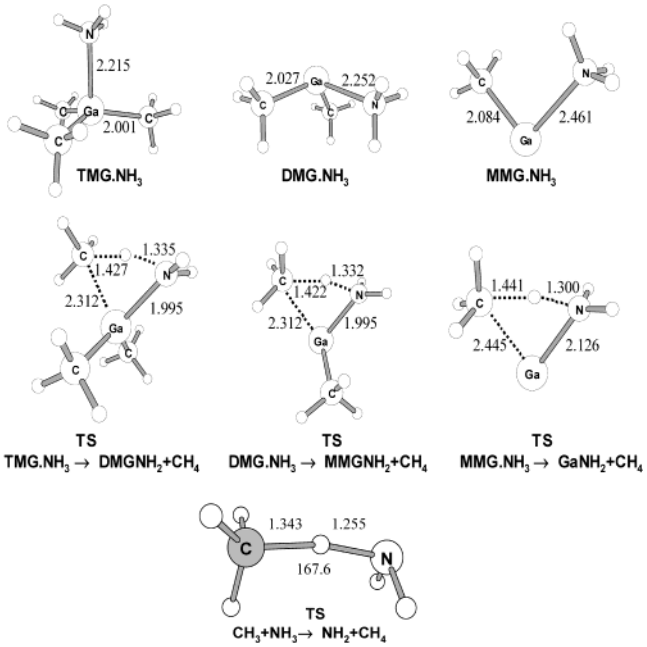

Figure 1. Molecular structures of the adducts and transition states of for CH_4 elimination. Unlabeled atoms are hydrogen. Bond lengths and angles are in angstroms and degrees, respectively.

The activation barriers of such reactions for TMG, DMG, and MMG are shown in Table 1. The activation barrier for CH_4 elimination decreases from TMG to MMG. The above reactions are chemically activated, because the energy released during the adduct formation can be utilized to cross the barrier for the CH_4 elimination process. As will be seen later, the adduct can only be stabilized by the collision of the carrier gas. The rate of adduct formation is, therefore, pressure-dependent. Figure 1 shows the structures of the adducts and the transition states for methane elimination. At the transition state, one of the Ga−C and N−H bonds is elongated while the Ga−N bond lengths are decreased from their original values in the complex. Almond et al.[21] have reported the experimental structure of the $TMG{\cdot}NH_3$ adduct by using gas phase electron diffraction method. Their reported values for Ga−C and Ga−N bonds are 1.979 and 2.161 Å, respectively. Figure 1 shows that our calculated bond lengths are in good agreement with the experiments.

One of the most important reactions in the MOVPE of GaN is the decomposition of TMG. TMG can decompose to Ga and CH_3 via successive elimination of three methyl groups as:

$$Ga(CH_3)_3 \rightarrow Ga(CH_3)_2 + CH_3 \rightarrow GaCH_3 + 2CH_3 \rightarrow Ga + 3CH_3$$

The lowest electronic states of TMG, DMG, and MMG are

singlet, doublet, and singlet, respectively. The present calculation shows that the above decomposition processes are direct, and the energy increases monotonically as the Ga−C bond is stretched. Therefore, activation barriers for decomposition are the dissociation energies of the corresponding Ga−C bonds. The dissociation energies are shown in Table 1. The values reported by Jacko and Price[22] agree quite well with those calculated using JANNAF data. Values calculated using quantum chemistry agree reasonably well with those reported by Jacko and Price, and the ones calculated using JANNAF data, except the MMG → Ga + CH_3 reaction. The activation barrier obtained using quantum chemistry for MMG → Ga + CH_3 is low as compared to the values reported by Jacko and Price. It is suspected that the energy of the Ga atom is underestimated in the present calculation.

Once the CH_3 radical is formed, it can react with NH_3 to produce NH_2 and CH_4 via a hydrogen abstraction reaction:

$$CH_3 + NH_3 \rightarrow CH_4 + NH_2$$

The transition structure for the above reaction is shown in Figure 1. At the transition state, the N···H···C moiety is bent. The activation barrier for this reaction is only 12 kcal/mol, and the reaction is almost thermoneutral. The calculated activation barrier agrees well with the experimental value of 10 kcal/mol.[23] The reported heat of reaction for this reaction at 298 K is 0.3 kcal/mol.[24] Assuming that the thermal correction to the reaction energy at 0 K is small, the calculated value is in good agreement with the experimental value.

Rate Constant Calculations. For the unimolecular decomposition reaction, the QRRK method was used. All rate constant calculations were performed using the code KWANT-RATE.[25] For comparison, the rate constants were also calculated using transition state theory. These reactions are thermally activated via the collision among the gas molecules and can be represented as

$$A + M \rightarrow A^* + M$$

$$A^* + M \rightarrow A + M$$

$$A^* \rightarrow \text{products}$$

A is a molecule that undergoes unimolecular decomposition, A* is the vibrationally activated A, and M is the third body, which can be the reactants, products, and/or inert gas. In the QRRK calculation, all above steps are taken into account, and the reaction must be pressure-dependent because the activation of A and deactivation of A* occur due to collision. On the other hand, rate constants using transition state theory (or Arrhenius expression) are the high-pressure limit to those calculated using unimolecular theories, such as QRRK and RRKM.[12] A detailed discussion of the QRRK theory is beyond the scope of this paper but can be found in references 12 and 13. As mentioned earlier, these decomposition reactions are direct and no specific transition state is involved during decomposition. To use the QRRK theory, one needs to know the high-pressure Arrhenius preexponential factor.[12] Therefore, the entropy of activation must be calculated. It is straightforward to calculate the entropy of activation for reactions with specific transition states using statistical thermodynamics, by calculating the partition function of the transition state and the equilibrium structure. In the case of a direct decomposition, there is no specific transition state, and no optimized transition structure can be obtained via quantum chemistry calculation. Therefore, one has to approximate a transition structure. Because these processes involve direct dissociation, the approximate transition structure will be very close to the dissociated product side on the potential energy surface. We therefore followed the method by Benson.[26] According to Benson, the bond distance of the breaking bond is approximately 2.5−3 times its equilibrium distance. Here, a value of 2.8 for TMG, DMG, and MMG decomposition has been used. The same value was used earlier by Wang and Pollard[27] for adsorption/desorption reactions. Because the approximate transition states of the decomposition reactions are "loose", one has to take into account the various degrees of freedoms of the transition states in order to calculate the entropy of activation accurately.[27,28] The following expression has been used to calculate the Arrhenius preexponential factor:

$$A = (e \cdot k_b T/h) \cdot \exp(\Delta S^{\#}/R) \qquad (1)$$

where k_b is the Boltzman constant, T is the temperature, h is the Planck constant, $\Delta S^{\#}$ is the entropy of activation, and R is the universal gas constant. Table 2 shows, as an example, the various degrees of freedom of TMG decomposition into DMG and CH_3. In this reaction, we assumed CH_3 groups as free rotors, and each nonlinear product fragment contributes to 3 degrees of rotation.[28] The correct identification of the various degrees of freedom of the reactant and transition state is crucial to obtaining the correct temperature variation of the preexponential factors. The preexponential factor for the recombination reaction (back reaction) is calculated from the equilibrium constant. The variation of the rate constant with pressure for TMG decomposition at 1000 K is shown in Figure 2. The rate constants show strong pressure dependence. Because the Arrhenius rate constant is the high-pressure limit of the unimolecular rate constant, the QRRK rate constant merges with the Arrhenius rate constant at high pressure. It is important to note that the

TABLE 2: Various Degrees of Freedom of the Reactant Transition State and Products for the TMG → DMG + CH_3 Reaction[a]

degrees of freedom	TMG	transition state	DMG + CH_3
vibration	30	25	25
internal rotation	3	7	2
external rotation	3	3	6
translation	3	3	6
total	39	38	39

[a] Note that the transition state has one less degree of freedom than the reactant and products.

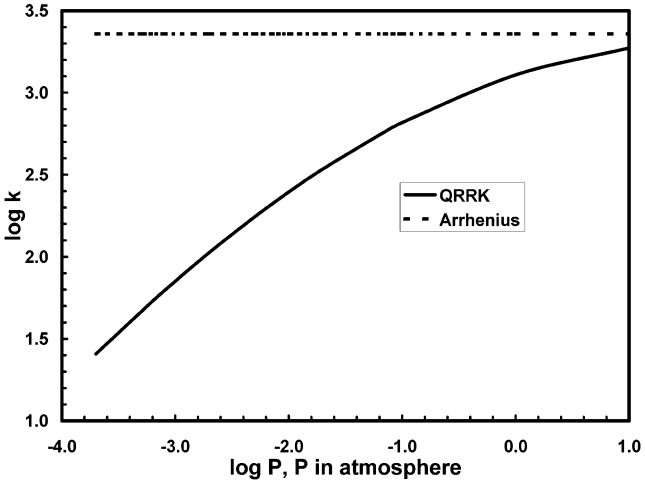

Figure 2. Variation of rate constant for TMG → DMG + CH_3 reaction with pressure. Note that at higher pressure, the QRRK rate constant converges to the transition state theory rate constant.

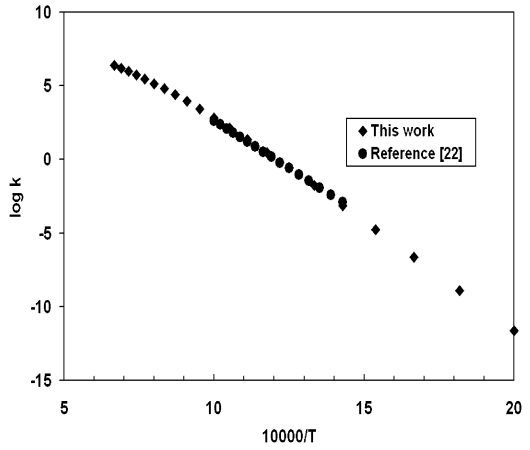

Figure 3. Comparison of calculated rate constant (using QRRK theory) with experiment for the reaction TMG → DMG + CH_3 at 0.1 atm pressure.

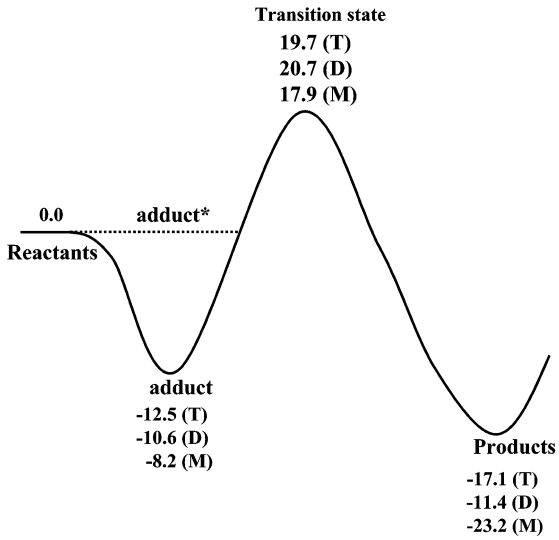

Figure 4. Potential energy diagram of for the TMG + NH_3 (T), DMG + NH_3 (D), amd MMG + NH_3(M) reactions. Energies are expressed in kcal/mol. The "adduct*" refers to the chemically activated adduct.

rate constant for the pressure-dependent reactions must be calculated at a pressure in which the MOVPE reactor operates. These rate constants were also calculated as a function of temperature at a pressure that was usually used in MOVPE reactor (approximately 0.1 atm). Figure 3 shows a comparison between the experimental results of Jacko and Price[22] with the present calculation, and we found excellent agreement.

The rate constants for reactions that proceed via adduct formation followed by CH_4 elimination (such as reactions of TMG, DMG, and MMG with NH_3) are calculated using the QRRK theory as well. Figure 4 shows the potential energy diagram of these reactions. The adduct is chemically activated (shown as "adduct*" in Figure 4) during the energy release of its formation. In a chemically activated process, all adduct molecules will have an energy that is equal to or greater than the energy released due to its formation. This energy is stored in the quantized vibrational level of the adducts and a portion of this energy can be utilized to cross the activation of the following processes. On the other hand, in a thermally activated reaction (such as unimolecular decomposition of TMG), the molecule gain energy via collision to overcome the activation barrier, in contrast to the chemically activated reaction where energy is gained via a previous chemical reaction. Therefore, an energetically "cold" adduct is expected to react much slower

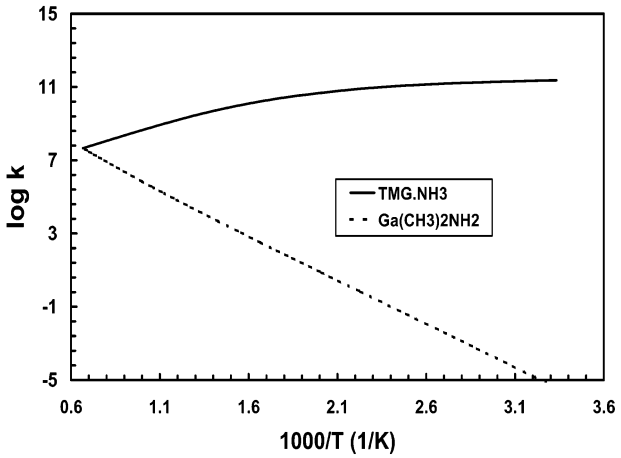

Figure 5. Variation of rate constants for the formation of the TMG·NH_3 adduct and $Ga(CH_3)_2NH_2$ with temperature at 0.1 atm pressure for the TMG + NH_3 reaction.

than the adduct, which is chemically activated. The chemically activated processes are frequently used in modeling combustion reactions[29] but have rarely been used in the MOVPE community. A detailed discussion about the chemically activated reactions can be found in the literature.[12,13] The activated adduct can only be stabilized by collision with other gas molecules; therefore, the rate constant for stabilized adduct formation is pressure-dependent. The stabilization of the adduct again competes with the reaction that eliminates CH_4. Therefore, the adduct formation and elimination of CH_4 from the adduct cannot be considered as a juxtaposition of these independent reactions. They must be treated simultaneously, and the rate constants have to be calculated using the concept of chemical activation. This fact has always been neglected in the past studies where these reactions have been treated as two independent reactions, and the adduct has not been considered as chemically activated.[5,30] Figure 5, as an example, shows the variation of the rate constants with temperature for reactions of NH_3 with TMG at 0.1 atm using H_2 as the carrier gas. It should be pointed out that the nature of the carrier gas has almost negligible effect on the rate constant calculated within the range of temperature and pressure in this work. The salient feature of these reactions is the rate constant for adduct formation decreases with an increase in temperature. On the other hand, the rate constants for CH_4 elimination increase sharply from a very low value. This is due to fact that the fraction of the energized adduct with energy equal or higher than the activation barrier for CH_4 elimination increases rapidly with temperature. Therefore, at higher temperatures, the probability of CH_4 formation via barrier crossing increases. At approximately 1700 K, the CH_4 elimination process becomes almost equal to that of adduct stabilization. However, this temperature is much higher as compared to the typical growth temperature of GaN, which is approximately 1000 K. At lower temperatures, stabilization of the energized adduct is the only predominant reaction channel, and as the temperature increases, the CH_4 elimination channel opens up at the cost of stabilization of the adduct. The correct variation of the rate constant with temperature is extremely important since the temperature of the substrate, on which GaN is deposited, is usually kept high, and there is a strong temperature gradient from the substrate to the bulk of the MOVPE reactor. Therefore, the species concentration close to the surface will strongly depend on the temperature variation of the rate constants. A similar procedure was used earlier for calculation of gas phase reaction related to gallium arsenide deposition.[31] Since it was

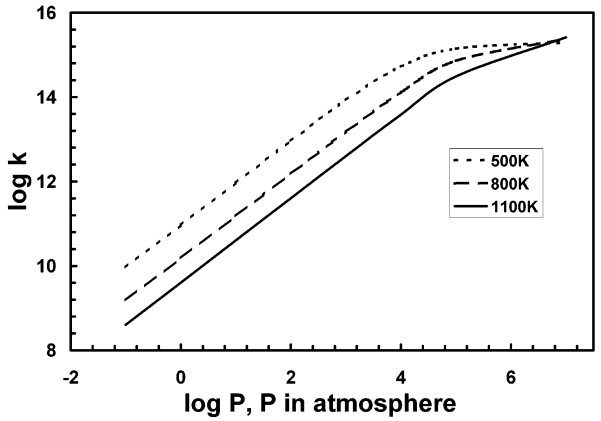

Figure 6. Variation of rate constant for the TMG·NH_3 adduct formation (via the TMG + NH_3 reaction) with pressure at three different temperatures.

TABLE 3: Gas Phase Reactions Considered for GaN MOVPE[a]

	reactions	*A*	*n*	*E*/*R*
G1	TMG ↔ DMG + CH_3	1.0×10^{47}	−9.18	38 750
G2	DMG ↔ MMG + CH_3	7.67×10^{43}	−9.8	17 120
G3	MMG ↔ Ga + CH_3	1.68×10^{30}	−5.07	42 290
G4	TMG + NH_3 → TMG·NH_3	2.28×10^{34}	−8.31	1568
G5	TMG + NH_3 → $(CH_3)_2GaNH_2$ + CH_4	1.7×10^{4}	2.0	10 050
G7	DMG + NH_3 → DMG·NH_3	4.08×10^{31}	−7.03	1628
G8	DMG + NH_3 → CH_3GaNH_2 + CH_4	5.30×10^{5}	1.56	10 440
G9	MMG + NH_3 → MMG·NH_3	7.95×10^{24}	−5.21	1054
G10	MMG + NH_3 → $GaNH_2$ + CH_4	8.10×10^{5}	1.3	8919
G11	NH_3+CH_3↔ NH_2 + CH_4	3.31×10^{3}	2.51	4962

[a] Rate constants for unimolecular and bimolecular reactions are expressed as s^{-1} and $cm^3/(mol\ s)$, respectively. Backward rates are calculated from equilibrium.

proposed that $(CH_3)_2GaNH_2$ is the precursor for the formation of the ring compound, the concentration of this species is expected to dictate the possibility of formation of the ring compound. Therefore, the above reaction rate constants will be utilized to calculate the concentration of the $(CH_3)_2GaNH_2$ species at different conditions. Figure 6 shows the variation of the rate constant for stabilization of the TMG·NH_3 adduct as a function of pressure at different temperatures. It shows that with an increase in pressure, the stabilization increases. At a lower pressure region, the rate constant is linearly dependent with pressure while at higher pressure the curve tends to flatten. At sufficiently high pressure, the rate constant becomes pressure-independent. Calculations show that the CH_4 elimination channel almost shuts off at high pressure. This is due to the fact that almost all energized adducts are stabilized at high-pressure limit, and the number of adducts with energies higher than the CH_4 elimination barrier is negligible. Figure 6 also shows that as the temperature increases, the high-pressure limits shift toward higher pressures. At higher temperatures, the number of energized adducts with energies higher than the activation barrier for the CH_4 elimination channel gradually increases, and more pressure is necessary to stabilize them. A very similar behavior is observed for MMG + NH_3 and DMG + NH_3 reactions. The temperature variations of the rate constants were finally fitted to the modified Arrhenius expression (i.e., $k = A \cdot T^n \exp(-E/RT)$] at 0.1 atm pressure, which is typical for MOVPE of GaN. The reactions and fitted rate constants are shown in Table 3.

We performed a perfectly stirred reactor (PSR) analysis by solving the following set of ordinary differential equation:

$$d[A_i]/dt = R_i$$

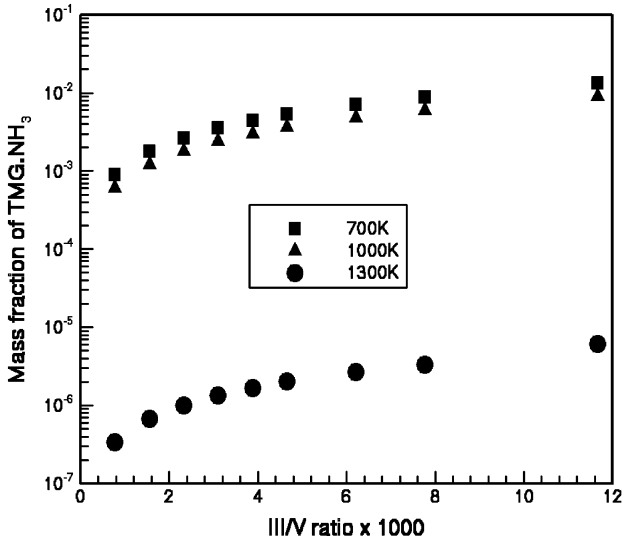

Figure 7. Variation of TMG·NH_3 mass fraction with III/V ratio at different temperatures. Rate constants shown in Table 3 are used for mass fraction calculations.

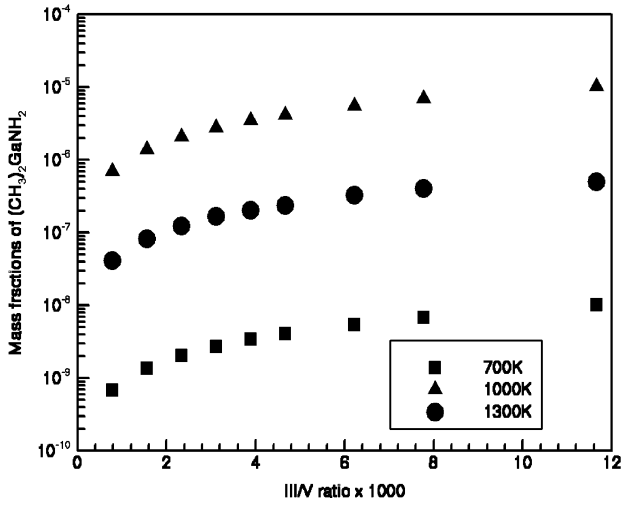

Figure 8. Variation of $(CH_3)_2GaNH_2$ mass fraction with III/V ratio at different temperatures. Rate constants shown in Table 3 are used for mass fraction calculations.

where A_i is the concentration of the ith species and R_i is the reaction rate that is computed using the rate constants shown in Table 3. In each case, the solutions were taken to steady state. These differential equations were solved at three different temperatures, say 700, 1000, and 1300 K, by varying TMG/NH_3 or III/V molar ratio at 0.1 atm pressure. In these calculations, we have assumed that TMG and NH_3 are inside a closed container with no carrier gas present (i.e., PSR). This essentially means that the concentrations of the species that are resulting from the reactions between TMG and NH_3 are the maximum possible. Figures 7 and 8 show the variation of TMG·NH_3 and $(CH_3)_2GaNH_2$ mass fractions with temperature and III/V ratio. As the TMG concentration increases, mass fractions of both species increase. This is due to the fact that the reaction rate between TMG and NH_3 increases. Most importantly, the mass fraction of $(CH_3)_2GaNH_2$, the precursor for the formation of the ring compound, remains always low. This concludes that ring formation in the gas phase is negligible and cannot contribute to the growth of GaN. Our conclusion is in agreement with the recent mass spectrometric studies by Bergman et al.[10]

Figures 7 and 8 also show some interesting features. The TMG·NH_3 mass fraction decreases with the increase in tem-

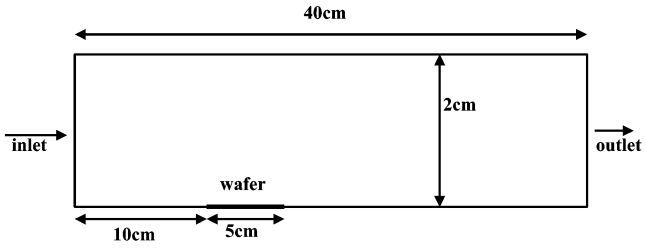

Figure 9. Reactor geometry and boundary conditions[32] used for the calculation of growth rate at different temperatures using CFD-ACE+.

perature while the $(CH_3)_2GaNH_2$ mass fraction increases from 700 to 1000 K but decreases at 1300 K. This due to the fact that there are two ways that TMG·NH_3 can disappear (i) formation of $(CH_3)_2GaNH_2$ via CH_4 elimination and (ii) unimolecular decomposition of TMG. At lower temperature (700 K), barriers for these two processes are hardly crossed, and TMG·NH_3 mass fraction is the largest and $(CH_3)_2GaNH_2$ is the lowest. At 1000 K, some TMG·NH_3 has accumulated enough energy to cross the activation barrier for the formation of $(CH_3)_2GaNH_2$. Therefore, the mass fraction of TMG·NH_3 decreases with an increase in the formation of $(CH_3)_2GaNH_2$. At very high temperatures, TMG undergoes unimolecular decomposition, which reduces the formation of both TMG·NH_3 and $(CH_3)_2GaNH_2$.

To explore the possibility of ring formation, we also performed simulation with the gas phase reactions shown in Table 3 using experimental reactor reported by Chen et al.[32] The geometry of the reactor is shown in Figure 9. The precursors, TMG and NH_3, are injected into the reactor through the inlet, and H_2 has been used as the carrier gas. The wafer is kept at 1200 K, and the pressure of the reactor is 0.1 atm. To solve the species concentration and temperature at different positions in the reactor, a set of coupled partial differential equations (such as the mass balance equation, momentum equation, enthalpy equation, and species mass fraction equation) are solved using the computational fluid dynamics (CFD) technique. The detailed discussion of the theory and method is out of the scope of this paper but can be found in the literature.[33] The calculations were performed using the commercial software CFD-ACE+ of CFD Research Corporation.[34] Figure 10 shows the calculated temperature and mass fractions distribution of various species within the reactor using the calculated rate constants. Figure 10a shows that the wafer, which is kept isothermally at 1200 K, heats the gas via conduction and convection. Figure 10b shows that the mass fraction of the

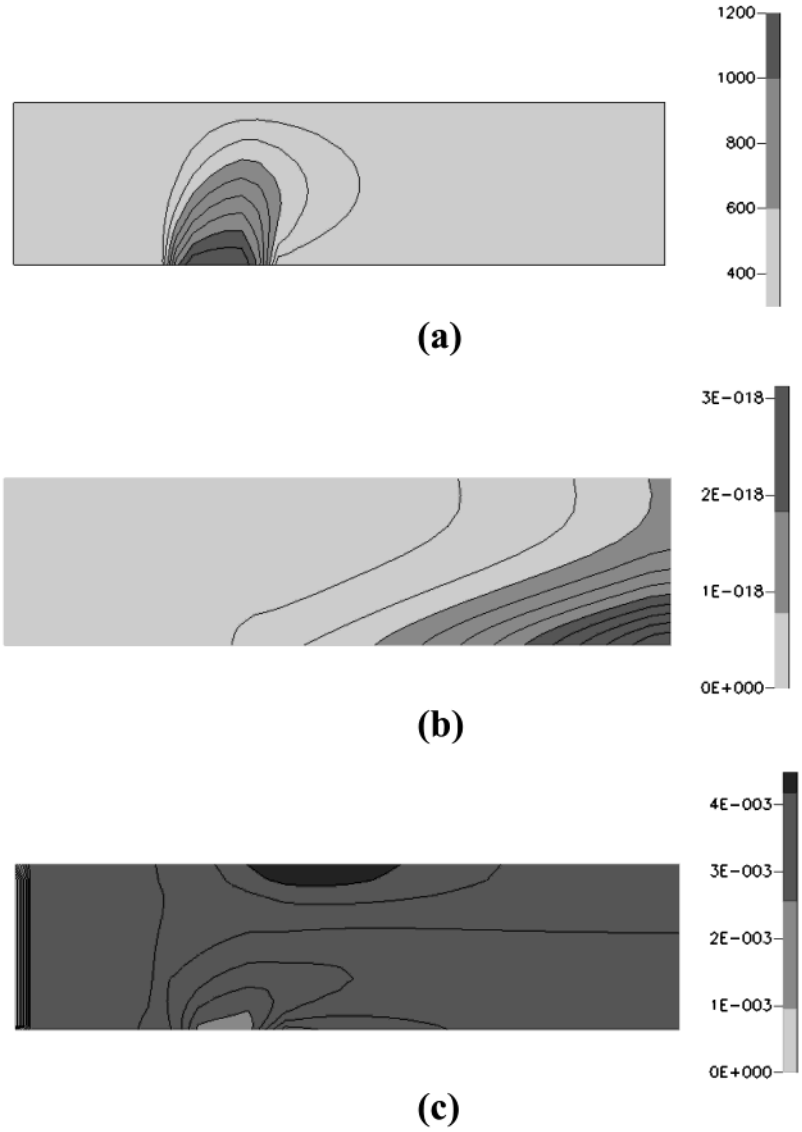

Figure 10. (a) Temperature distribution inside the reactor when the wafer is kept at 1200 K; (b) mass fraction of $Ga(CH_3)_2NH_2$ and (c) mass fraction of the adduct TMG·NH_3.

$Ga(CH_3)_2NH_2$ is negligible. We therefore conclude that the possibility for the formation of ring compound is also almost negligible in the actual growth condition of GaN. Figure 10c shows that the major intermediate species is $TMG{\cdot}NH_3$ adduct, and it forms mostly in the cold region of the reactor. At the hot region, this TMG and the complex break into the other products, which lead to the depletion of $TMG{\cdot}NH_3$.

Conclusions

The ring compound, $[Ga(CH_3)_2NH_2]_3$, so far has been believed to be the major species for growth of a GaN thin film. However, there is no concrete experimental evidence to support such a postulate. We have performed DFT calculations followed by rate constant calculations via QRRK theory in order to resolve this issue. The rate constants were used for calculating the concentration of the monomer, $Ga(CH_3)_2NH_2$, which is the precursor for the ring compound, over a wide range of temperatures and III/V ratios. Our calculations showed that the monomer concentration is almost negligible. We therefore conclude that ring compound hardly contributes to the growth of GaN. Our results are in agreement with the recent mass spectrometric studies.

Acknowledgment. This work is funded by National Science Foundation under the Phase II SBIR (DMI 9983415; program officer, Ms. Jean Bonney). I thank Dr. S. Mazumder of CFDRC for many helpful discussions and Dr. R. Sumathi of MIT for a discussion on rate constant calculation. I also thank Professor J. B. Adams for providing computer resources.

References and Notes

(1) Stringfellow, G. B. *Organometallic Vapor-Phase Epitaxy: Theory and Practice*, 2nd ed.; Academic Press: New York, 1999.

(2) Kisker, D.; Kuech, T. F. *The Principles and Practice of Organometallic Vapor Phase Epitaxy*; Elsevier Science: Amsterdam, 1993; Vol. 3.

(3) Kisker, D. W.; Kuech, T. F. *Handbook on Semiconductors*, 2nd ed.; Elsevier Science: Amsterdam, 1994; Vol. 4.

(4) Thon, A.; Kuech, T. F. *Appl. Phys. Lett.* **1996**, *69*, 55.

(5) Mihopoulos, T. Reaction and Transport Processes in OMCVD: Selective and Group III−Nitride Growth, M. I. T., 1999.

(6) Theodorpoulos, C.; Mountziaris, T. J.; Moffat, H. K.; Han, J. *J. Cryst. Growth* **2000**, *217*, 65.

(7) Safvi, S. A.; Redwing, J. M.; Tischler, M. A.; Kuech, T. F. *J. Electrochem. Soc.* **1997**, *144*, 1789.

(8) Sun, J.; Redwing, J. M.; Kuech, T. F. *Phys. Status Solidi A* **1999**, *176*, 693.

(9) Almond, M. J.; Drew, M. G. B.; Jenkins, C. E.; Rice, D. A. *J. Chem. Soc., Dalton Trans.* **1992**, 5.

(10) Bergman, U.; Reimer, V.; Atakan, B. *Phys. Chem. Chem. Phys.* **1999**, *1*, 5593.

(11) Mazzarese, D.; Tripathi, A.; Conner, W. C.; Jones, K. A.; Calderon, L.; Eckart, D. W. *J. Electron. Mater.* **1989**, *18*, 369.

(12) Robinson, P. J.; Holbrook, K. A. *Unimolecular Reactions*; Wiley-Interscience: New York, 1972.

(13) Dean, A. M. *J. Phys. Chem.* **1985**, *89*, 4600.

(14) Sengupta, D.; Chandra, A. K. *J. Chem. Phys.* **1994**, *101*, 3906.

(15) Nguyen, M. T.; Sengupta, D.; Vanquickenborne, L. G. *J. Phys. Chem.* **1996**, *100*, 10956.

(16) Frisch, M. J.; Trucks, G. W.; Schlegel, H. B.; Scuseria, G. E.; Robb, M. A.; Cheeseman, J. R.; Zakrzewski, V. G.; Montgomery, J. A., Jr.; Stratmann, R. E.; Burant, J. C.; Dapprich, S.; Millam, J. M.; Daniels, A. D.; Kudin, K. N.; Strain, M. C.; Farkas, O.; Tomasi, J.; Barone, V.; Cossi, M.; Cammi, R.; Mennucci, B.; Pomelli, C.; Adamo, C.; Clifford, S.; Ochterski, J.; Petersson, G. A.; Ayala, P. Y.; Cui, Q.; Morokuma, K.; Malick, D. K.; Rabuck, A. D.; Raghavachari, K.; Foresman, J. B.; Cioslowski, J.; Ortiz, J. V.; Stefanov, B. B.; Liu, G.; Liashenko, A.; Piskorz, P.; Komaromi, I.; Gomperts, R.; Martin, R. L.; Fox, D. J.; Keith, T.; Al-Laham, M. A.; Peng, C. Y.; Nanayakkara, A.; Gonzalez, C.; Challacombe, M.; Gill, P. M. W.; Johnson, B. G.; Chen, W.; Wong, M. W.; Andres, J. L.; Head-Gordon, M.; Replogle, E. S.; Pople, J. A. *Gaussian 98*, revision A.9; Gaussian, Inc.: Pittsburgh, PA, 1998.

(17) Lee, C.; Yang, W.; Parr, R. G. *Phys. Rev. B* **1988**, *37*, 785.

(18) Hay, P. J.; Wadt, W. R. *J. Chem. Phys.* **1985**, *82*, 299.

(19) Nakamura, K.; Makino, O.; Tachibana, A.; Matsumoto, K. *J. Organomet. Chem.* **2000**, *611*, 514.

(20) Watwe, R. M.; Dumesic, J. A.; Kuech, T. F. *J. Cryst. Growth* **2000**, *221*, 751.

(21) Almond, M. J.; Jenkins, C. E.; Rice, D. A.; Hagen, K. *J. Organomet. Chem.* **1992**, *439*, 251.

(22) Jacko, M. G.; Price, S. J. W. *Can. J. Chem.* **1963**, *41*, 1560.

(23) Arthur, N. L.; Bell, T. N. *Rev. Chem. Intermed.* **1978**, *2*, 37.

(24) NIST Chemistry web book; Vol. 2002; http://webbook.nist.gov/chemistry.

(25) Sengupta, D.; Nguyen, K. A. KWANT_RATE, version 1 ed.; Leuven, 1996.

(26) Benson, S. W. *Thermochemical Kinetics*, 2nd ed.; John Wiley and Sons: New York, 1976.

(27) Wang, Y.-F.; Pollard, R. *J. Electrochem. Soc.* **1995**, *142*, 1712.

(28) Gilbert, R. G.; Smith, S. C. *Theory of Unimolecular and Recombination Reactions*; Blackwell Scientific Publications: London, 1990.

(29) Yu, C. L.; Wang, C.; Frenklach, M. *J. Phys. Chem.* **1995**, *99*, 14377.

(30) Mountziaris, T. J.; Jensen, K. F. *J. Electrochem. Soc.* **1991**, *138*, 2426.

(31) Tirtowidjojo, M.; Pollard, R. *J. Cryst. Growth* **1989**, *98*, 420.

(32) Chen, C. H.; Liu, H.; Steigerwald, D.; Imler, W.; Kuo, C. P.; Craford, M. G.; Ludowise, M.; Lester, S.; Amano, J. *J. Electron. Mater.* **1996**, *25*, 1004.

(33) Versteeg, H. K.; Malasekara, W. *An Introduction to Computational Fluid Dynamics*; Prentice Hall: London, 1995.

(34) CFD-ACE+; version 6.6; Huntsville, AL.

(35) Chen, Q.; Dapkus, P. D. *J. Electrochem. Soc.* **1991**, *138*, 2821.